ChemPubSoc Europe

DOI: 10.1002/chem.201403315

CHEMISTRY A European Journal Full Paper

Supramolecular Chemistry

# Near-Infrared Croconaine Rotaxanes and Doped Nanoparticles for Enhanced Aqueous Photothermal Heating

Graeme T. Spence,[a] Shun Shang Lo,[a] Chenfeng Ke,[b] Harry Destecroix,[b] Anthony P. Davis,[b] Gregory V. Hartland,[a] and Bradley D. Smith*[a]

**Abstract:** The photothermal effect is the generation of heat by molecules or particles upon high-energy laser irradiation, and near-infrared absorbers such as gold nanoparticles and organic dyes have a range of potential photothermal applications. The favourable photothermal properties of thiophene-functionalised croconaine dyes were recently discovered. The synthesis and properties of novel croconaine rotaxane and pseudorotaxane architectures capable of efficient photothermal performance in both organic and aqueous environments are reported. The versatility of this dye-encapsulation strategy was demonstrated by the preparation of two organic croconaine rotaxanes using different synthetic methods: the formation of an aqueous pseudorotaxane association complex, and the synthesis of water-soluble, croconaine-doped silicated micelle nanoparticles. All of these near-infrared-absorbing systems exhibit excellent photothermal behaviour, with pseudorotaxane and rotaxane formation vital for effective aqueous heat generation. Dye encapsulation provides steric protection to enhance the stability of a water-sensitive croconaine dye, while rotaxane-doped nanoparticles avoid detrimental band broadening caused by chromophore coupling.

## Introduction

There is increasing interest in developing methods of generating heat in nanoscale environments. The most common approach uses the photothermal effect, namely the absorption of laser light by molecules or particles that convert this energy into heat. Applications of nanoscale heat generation include photothermal cancer therapy,[1] photoacoustic imaging,[2] drug delivery,[3] tissue repair,[4] photothermal reactions,[5] and polymer welding.[6]

Gold nanoparticles are often used for photothermal studies owing to their tuneable surface plasmon resonance bands,[7] but there are potential concerns for certain types of biological applications owing to slow rates of diffusion and clearance in vivo. Although organic dyes can compete with gold nanoparticles on a heat generation per mass basis,[8] many near-infrared (NIR) organic dyes suffer greatly from photobleaching. Therefore, there is a need to develop alternative, photostable NIR chromophores with well-characterised photothermal properties, and recent studies have included metallo-naphthalocyanine, porphyrin, and cyanine derivatives.[6,9]

Recently, we discovered that thiophene-functionalised croconaine dyes,[10] such as the organic-solvent-soluble **1** (Figure 1), can act as high-performance NIR photothermal agents owing to their intense absorption around 800 nm, weak fluorescence, extremely low singlet oxygen photosensitisation, and importantly, high chemical and photothermal stability.[8a] These collective attributes compare favourably with the alternative NIR dye systems. Furthermore, we demonstrated that anthracene-based tetralactam macrocycle **2** can encapsulate croconaine dye **1** to form pseudorotaxane association complex **2⊃1**, which exhibits a red shift in the croconaine absorbance band. Herein, we describe detailed studies that use these building blocks to create three new types of croconaine architectures for photothermal heating. First, two permanently interlocked organic croconaine rotaxanes were prepared using "stoppering" and "clipping" strategies. Additionally, we report two methods of producing water-soluble croconaine systems. One method produced a mono-disperse pseudorotaxane association complex, and the other croconaine-doped silicated micelle nanoparticles. Crucially, pseudorotaxane or rotaxane formation was required in both of these water-soluble systems to solve dye stability or self-aggregation problems. All of the reported croconaine derivatives exhibit impressive photothermal performance and appear highly suited to various complementary photothermal applications.

[a] Dr. G. T. Spence, Dr. S. S. Lo, Prof. G. V. Hartland, Prof. B. D. Smith
Department of Chemistry and Biochemistry
University of Notre Dame, IN 46556 (USA)
E-mail: smith.115@nd.edu

[b] Dr. C. Ke, H. Destecroix, Prof. A. P. Davis
School of Chemistry
University of Bristol, BS8 1TS (UK)

Supporting information for this article is available on the WWW under http://dx.doi.org/10.1002/chem.201403315.

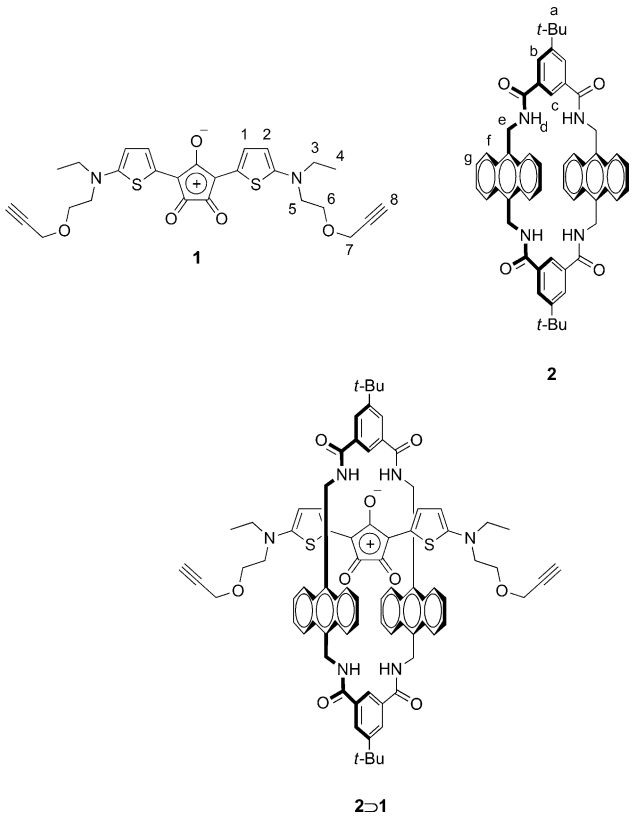


**Figure 1.** Previously reported croconaine dye **1**, macrocycle **2**, and pseudorotaxane **2⊃1**.[8a]

## Results and Discussion

### Organic-solvent-soluble croconaine rotaxanes

The two most frequent methods of rotaxane synthesis are stoppering and clipping.[11] Stoppering is achieved by covalent addition of sufficiently large stopper groups to a pseudorotaxane assembly, while clipping is the cyclisation of a macrocycle around a dumbbell-shaped axle. Both strategies were employed to prepare the first permanently interlocked rotaxanes containing croconaine dyes.

To realise the stoppering strategy, the copper-catalysed alkyne–azide cycloaddition (CuAAC), or click, reaction was utilised to convert alkyne-functionalised pseudorotaxane **2⊃1** into permanently interlocked rotaxane **3** (Figure 2; Supporting Information, Scheme S1). The product was isolated in 84% yield, and full characterisation of **3** was achieved using NMR, mass spectrometry, and photophysical methods (see below and the Supporting Information). Unlike pseudorotaxane **2⊃1**, which rapidly dissociates in polar organic solvents at room temperature, rotaxane **3** is completely stable in acetone, demonstrating that the terminal 3,5-*tert*-butylbenzene stopper groups have sufficient steric size to prevent dethreading (Supporting Information, Figure S45).

The alternative clipping approach employed tetra-substituted croconaine dye **4** as a dumbbell-shaped axle. Ten molar equivalents of 5-*tert*-butylisophthaloyl dichloride and 9,10-bis(aminomethyl)anthracene were reacted under high-dilution

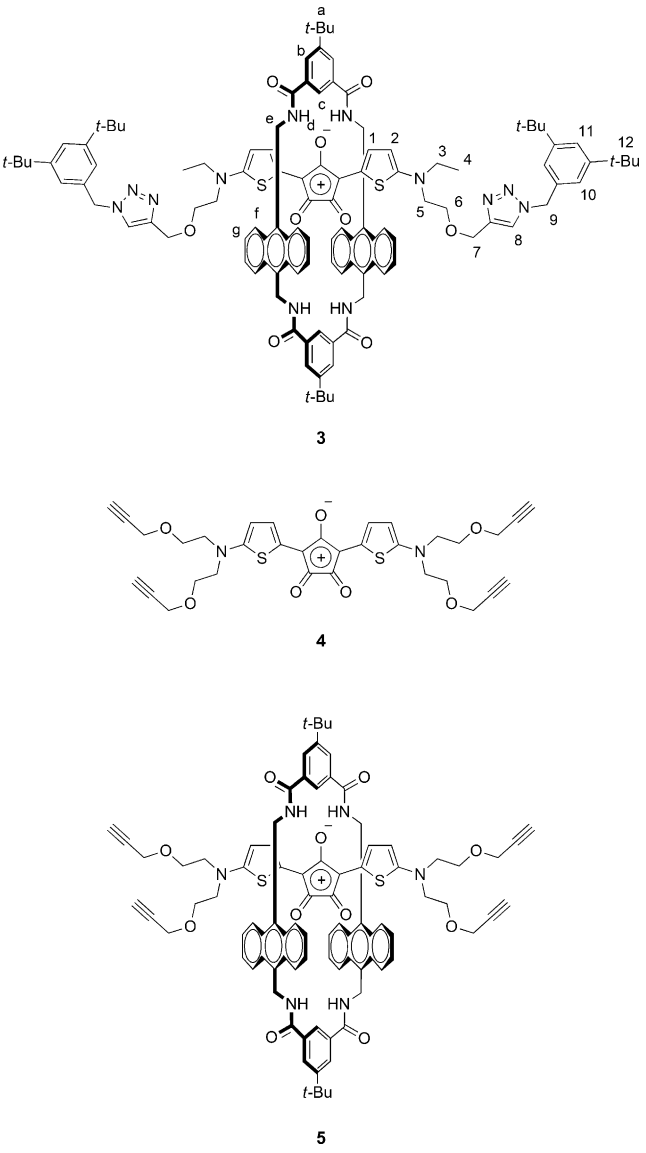


**Figure 2.** Stoppered croconaine rotaxane **3**, tetraalkyne dye **4**, and clipped rotaxane **5**.

conditions in the presence of one equivalent of dye **4**, affording target rotaxane **5** in 81% yield (Supporting Information, Scheme S2). The permanently interlocked structure of rotaxane **5** was again confirmed by its stability in polar organic solvents (Supporting Information, Figure S45).

Thiophene–croconaine derivatives exhibit conformational isomerism owing to their unsymmetrical structures (Figure 3a). The isomers are in slow exchange on the NMR timescale; for example, four signals are observed for both thiophene protons 2 in the $^1$H NMR spectrum of dye **1** (Figure 3b), with integration indicating two major isomers (*trans* and *cis*) and one minor (*cis*).[8a] The same conformational behaviour is observed for croconaine rotaxanes **3** and **5** (Figure 3a), as indicated by the peaks corresponding to isophthalamide protons b in rotaxane **3** (Figure 3c). The unsymmetrical croconaine de-symmetrises the two isophthalamide groups of the surrounding macrocycle, and six signals for protons b are observed corresponding

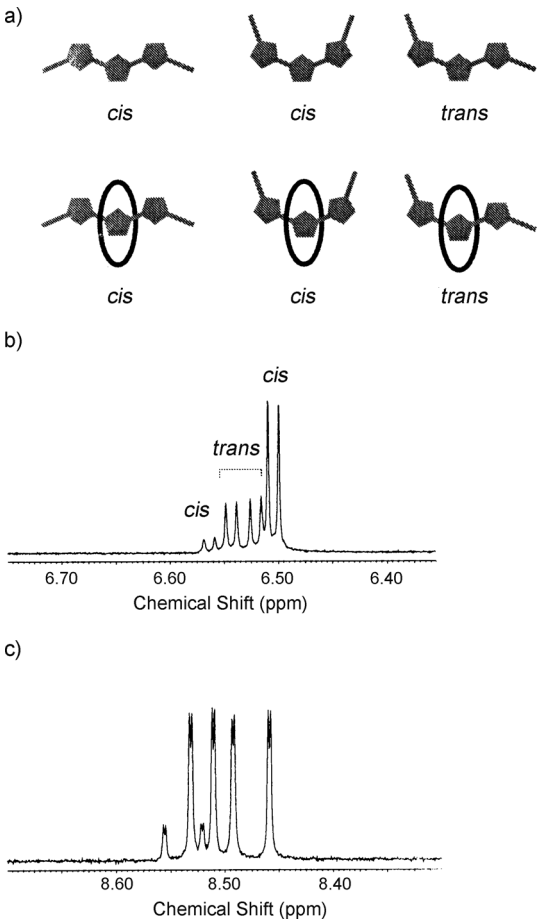


**Figure 3.** a) Conformational isomers of thiophene–croconaine dyes, such as **1** and **4**, and thiophene-croconaine rotaxanes, such as **3** and **5**. b) Region of the $^1$H NMR spectrum ($CDCl_3$, 600 MHz, 295 K) of croconaine dye **1** corresponding to thiophene protons 2 and c) region of the $^1$H NMR spectrum ($CDCl_3$, 600 MHz, 295 K) of croconaine rotaxane **3** corresponding to macrocycle protons b. See Figures 1 and 2 for atom labels.

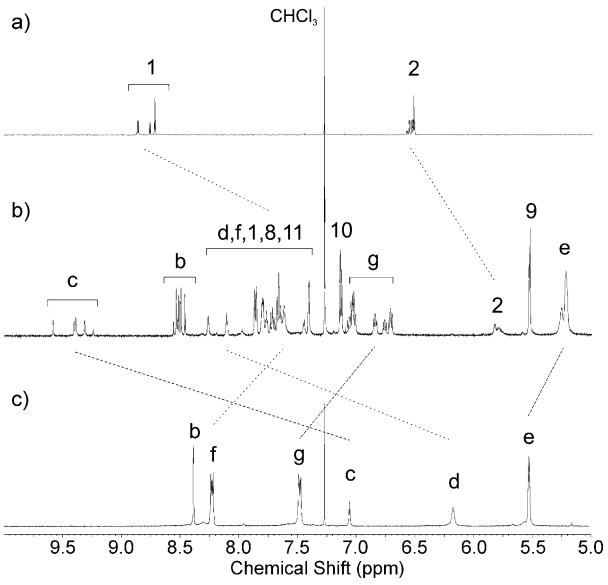


**Figure 4.** Diagnostic region of the $^1$H NMR spectra ($CDCl_3$, 600 MHz, 295 K) of a) croconaine dye **1**, b) croconaine rotaxane **3**, and c) macrocycle **2**.

**Table 1.** Photophysical data for croconaine dyes **1** and **4**, croconaine rotaxanes **3** and **5**, and macrocycle **2** ($CHCl_3$, 5.0 μM).

| | $\lambda_{abs,max}$ [nm] | $\varepsilon$ [$L\,mol^{-1}\,cm^{-1}$] | $\lambda_{ex,max}$ [nm] | $\lambda_{em,max}$ [nm] | $\Phi_f$[a] $\lambda_{ex}$ = 750 nm | $\Phi_f$[b] $\lambda_{ex}$ = 350 nm |
|---|---|---|---|---|---|---|
| Dye **1** | 795 | $2.9\times10^5$ | 764 | 811 | 0.06 | – |
| Dye **4** | 795 | $3.1\times10^5$ | 764 | 810 | 0.08 | – |
| Rotaxane **3** | 824 | $1.8\times10^5$ | 764 | 837 | 0.02 | 0.03 |
| Rotaxane **5** | 825 | $1.4\times10^5$ | 764 | 837 | 0.02 | 0.09 |
| Macrocycle **2** | – | – | – | – | – | 0.77 |

[a] Relative to indocyanine green in EtOH ($\Phi_f = 0.13$).[15] [b] Relative to 9,10-diphenylanthracene in cyclohexane ($\Phi_f = 0.93$).[16]

to the two major and one minor croconaine conformational isomers. Similar splitting is present for protons c (Supporting Information, Figure S37), and is also observed in the spectrum for rotaxane **5** (Supporting Information, Figure S40).[12]

Assignment of the $^1$H NMR spectra of rotaxanes **3** and **5** was aided by 2D $^1$H–$^1$H COSY and ROESY NMR (Supporting Information), and diagnostic $^1$H NMR shifts corresponding to rotaxane formation were observed for both systems (Figure 4; Supporting Information, Figure S18). Specifically, hydrogen bonding between the croconaine core and isophthalamide motifs produced downfield shifts in macrocycle proton signals c and d, while aromatic shielding induces upfield shifts in dye protons 1 and 2 and macrocycle protons e, f, and g.

The photophysical properties of dyes **1** and **4** and rotaxanes **3** and **5** are listed in Table 1. Upon rotaxane formation, a red-shift in the croconaine absorbance band of approximately 30 nm is observed with a concomitant reduction in molar absorptivity (Figure 5a; Supporting Information, Figure S44a). Previously, similar bathochromic shifts were observed for related squaraine rotaxane derivatives[13] and exploited for activated photothermal heating using croconaine pseudorotaxane **2**⊃**1**.[8a] Along with these absorption perturbations, comparison of quantum yields indicates that dye encapsulation has a moderate quenching effect on the already weak croconaine fluorescence emission ($\Phi_f$ values in Table 1, fluorescence spectra shown in Figure 5b and the Supporting Information, Figure S44b). Anthracene emission in rotaxanes **3** and **5** is also quenched in comparison with macrocycle **2**. This is consistent with energy transfer to the encapsulated croconaine component,[14] although other quenching processes are possible.

Laser-induced heat generation experiments were undertaken to determine whether the favourable photothermal behaviour of croconaine dye **1** was affected by macrocycle encapsulation. Two fundamental questions were addressed. Firstly, while our previous study confirmed that photothermal output is related to optical density and the Beer–Lambert law,[8a] it was important to determine the sensitivity of the bulk heating response to quenching of croconaine fluorescence emission upon encapsulation of dye **1** within rotaxane **3** ($\Phi_f = 0.06$ and 0.02 respectively). Secondly, as the photothermal effect has been shown to promote bond dissociation events,[3a,5] we were not

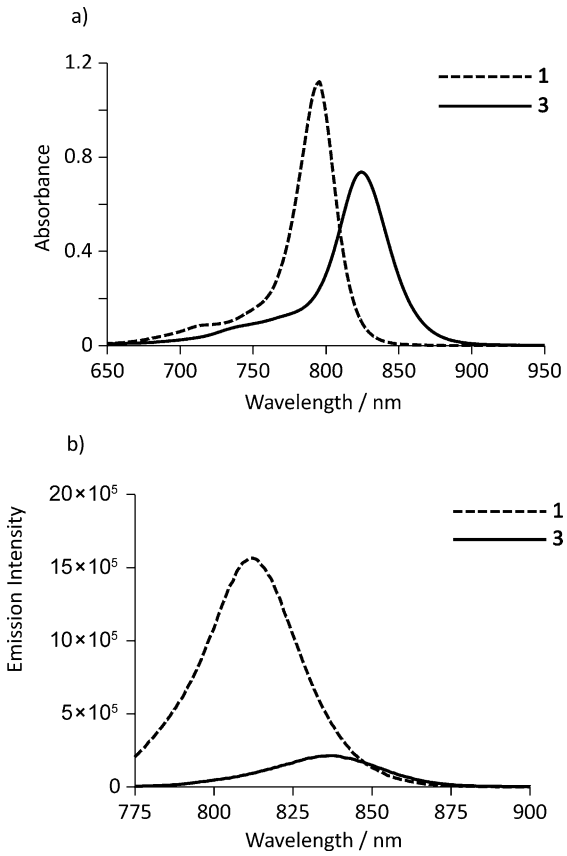


**Figure 5.** Comparative a) absorption spectra and b) fluorescence spectra for croconaine dye **1** and rotaxane **3** ($CHCl_3$, 5.0 μM, $\lambda_{ex}$ = 765 nm).

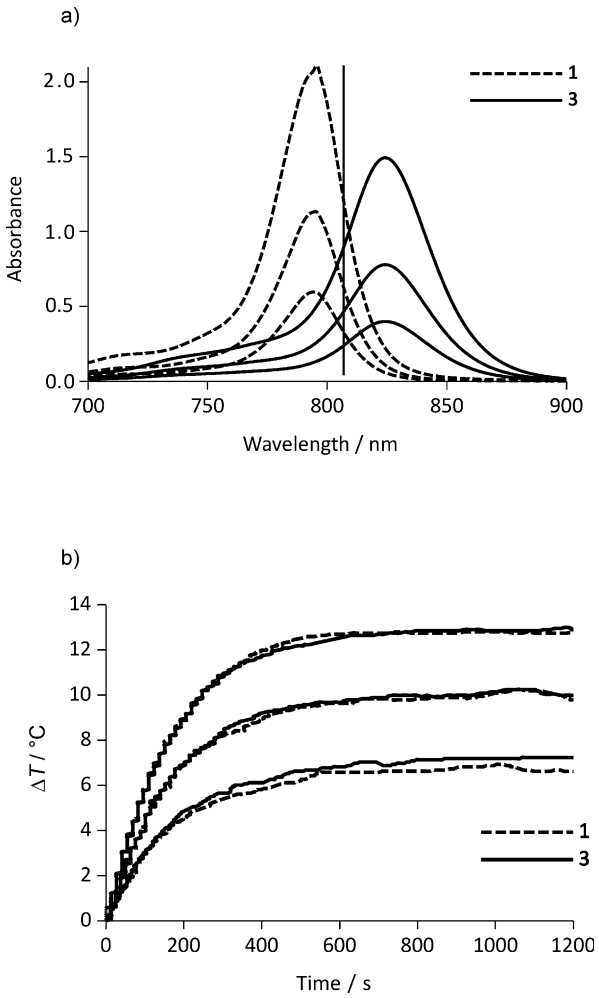


**Figure 6.** a) Absorption spectra for solutions of croconaine dye **1** and rotaxane **3** at different concentrations ($CHCl_3$), and b) the corresponding temperature change profiles observed during laser irradiation (808 nm, 250 mW).

sure if laser-induced heating would lead to dethreading of pseudorotaxane **2**⊃**1**.

To ascertain the effect of rotaxane formation on photothermal heat generation beyond the reduction in molar absorptivity seen in Figure 5a, the optical densities of different $CHCl_3$ solutions of dye **1** and rotaxane **3** were matched at 808 nm (Figure 6a). The solutions were irradiated for 20 min with 250 mW coherent light from an 808 nm laser diode, and the solution temperature was monitored using a thermocouple (Figure 6b). The lack of a significant difference between the heat generation profiles (Supporting Information, Table S3) indicates that the modest fluorescence quenching upon encapsulation does not appear to affect the photothermal efficiency of the croconaine chromophore. In other words, if optical densities are matched then the bulk photothermal output is identical for croconaine dye **1** and rotaxane **3**.

The stability of pseudorotaxane **2**⊃**1** was investigated by irradiating separate 5.0 μM solutions of **2**⊃**1** and **3** for 20 min with 250 mW, 820 nm coherent light from a tunable Ti:sapphire laser. The absorbance values of **2**⊃**1** and **3** were identical at this wavelength and no significant difference in the average temperature changes were observed: $\Delta T = 6.9 \pm 0.3\,^{\circ}C$ for **2**⊃**1**, and $6.7 \pm 0.2\,^{\circ}C$ for **3** (Figure S49). Furthermore, the absorption spectra of the solutions did not change upon laser irradiation (Supporting Information, Figure S50).[17] We conclude that organic-solvent-soluble croconaine pseudorotaxane **2**⊃**1** does not dissociate to any significant extent under photothermal heating.

### Water-soluble croconaine pseudorotaxane

To achieve aqueous photothermal heating, a water-soluble analogue of pseudorotaxane **2**⊃**1** was produced by encapsulating bis(guanidinium) croconaine dye **6** inside water-soluble macrocycle **7**[18] (Figure 7). Rapid association driven largely by the hydrophobic effect occurred upon addition of five molar equivalents of macrocycle **7** to dye **6**, signalled by the characteristic 30 nm red shift in croconaine absorbance (Figure 8a). Furthermore, while bis(guanidinium) dye **6** is unstable in water, with a 40% reduction in the croconaine absorbance band observed over 4 h (Figure 8b), pseudorotaxane **7**⊃**6** exhibits no instability.[19] Steric shielding of the croconaine core within the surrounding macrocycle is responsible for this protection effect.[13,20] The combination of rapid association and steric protection of the encapsulated croconaine supports the feasibility of future efforts to trigger pseudorotaxane formation for activated photothermal heat generation in water.

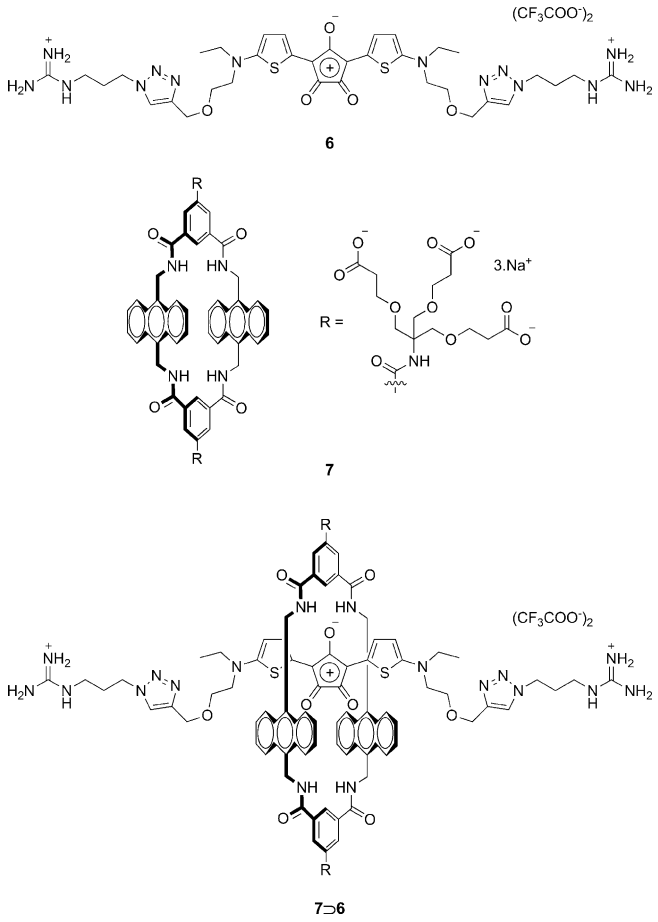


**Figure 7.** Water-soluble bis(guanidinium) croconaine dye **6**, macrocycle **7**, and pseudorotaxane **7⊃6**.

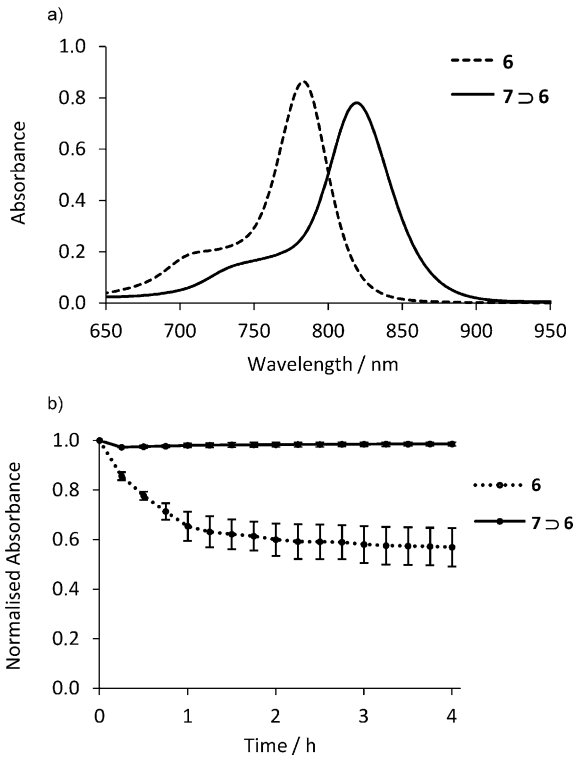


**Figure 8.** a) Absorption spectra of bis(guanidinium) croconaine dye **6** and pseudorotaxane **7⊃6** ($H_2O$, 5 μM), and b) changes in relative absorbance for **6** (784 nm) and **7⊃6** (818 nm) over 4 h ($n=3$, error bars correspond to standard errors). Note: **7⊃6** was formed in situ from dye **6** and 5.0 equivalents of macrocycle **7**.

The photothermal behaviour of water-soluble assembly **7⊃6** was investigated by exposing a solution to four cycles of laser irradiation (250 mW, 820 nm), and subsequent cooling (Figure 9). Importantly, the reproducibility of the heating response, and the lack of changes in the corresponding absorption spectrum (Supporting Information, Figure S52), demonstrates that **7⊃6** is an effective system for aqueous heat generation, and that unstable bis(guanidinium) dye **6** remains strongly encapsulated by the protective macrocycle **7** during laser-induced heating.

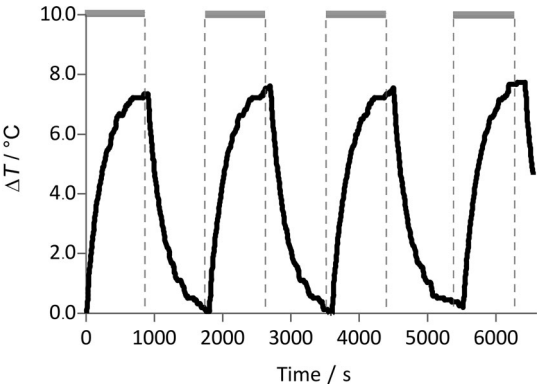


**Figure 9.** Temperature change profile observed for a solution of bis(guanidinium) croconaine pseudorotaxane **7⊃6** ($H_2O$, 5.0 μM) upon cycles of laser irradiation (250 mW, 820 nm, indicated by the bars at top) and subsequent cooling to room temperature.

### Water-soluble croconaine-doped nanoparticles

Croconaine-doped silicated micelle nanoparticles were synthesised by a known procedure that first encapsulates hydrophobic dyes within Pluronic micelle cores, and then forms permanent nanoparticles by silica deposition (Scheme 1).[21] The surface polyethylene glycol (PEG) chains impart excellent water solubility and biocompatibility. Croconaine dye **1**, rotaxane **3** (Figure 1), and dumbbell-shaped axle **8** (Figure 10) were used as dopants, and the resulting nanoparticles were characterised using DLS and absorption spectroscopy.

In agreement with previous reports using this method,[21] the synthesised nanoparticles had narrow size distributions with mean sizes around 15 nm (Figure 11 a; Supporting Information, Table S1). While the relative absorption spectra reveal that axle **8** and rotaxane **3** were efficiently encapsulated (Figure 11 b), only a very minor croconaine absorbance band was observed for the nanoparticles doped with dye **1**. Corresponding loading percentages of less than 5% for dye **1**, 40–50% for axle **8**, and 50–60% for rotaxane **3** were estimated. It is supposed that the increased hydrophobicity of **8** and **3** increased the extent of dye encapsulation within the Pluronic micelle

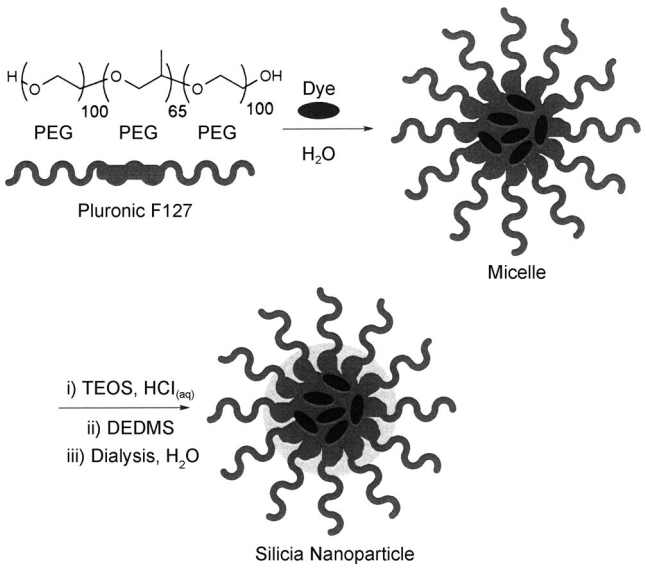


**Scheme 1.** Synthesis of dye-doped Pluronic micelles and the corresponding silicated nanoparticles. TEOS = tetraethyl orthosilicate, DEDMS = diethoxydimethylsilane.

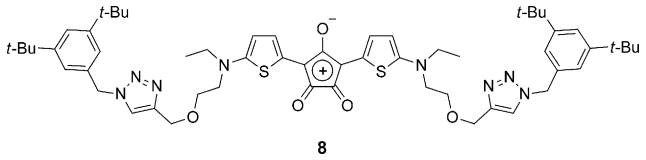


**Figure 10.** Dumbbell-shaped croconaine axle **8**.

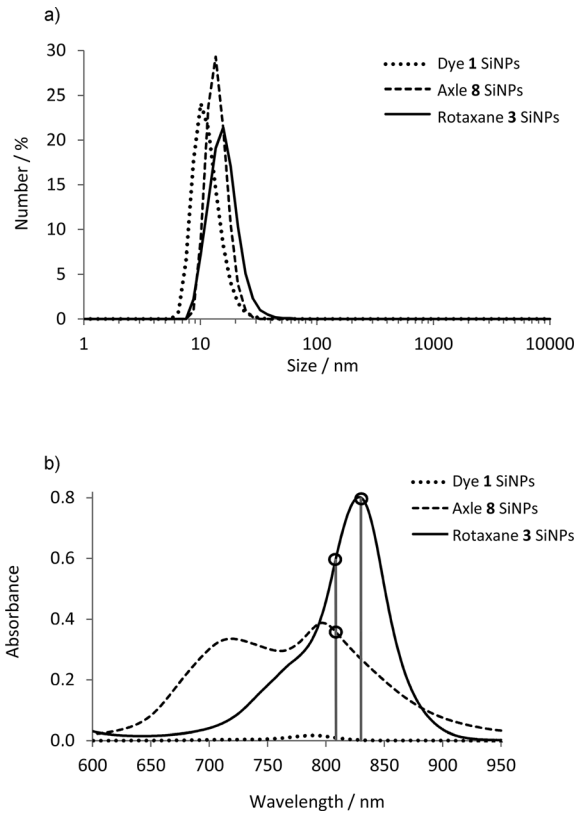


**Figure 11.** a) Dynamic light scattering (DLS) measurements and b) relative absorption spectra for solutions of silicated micelle nanoparticles (SiNPs) doped with croconaine dye **1**, axle **8**, or rotaxane **3** ($H_2O$). Relative absorbance values at the laser wavelengths (808 and 830 nm) are marked with black circles.

cores during nanoparticle synthesis. Furthermore, the absorbance band for the nanoparticles doped with axle **8** was severely broadened owing to croconaine self-aggregation, while the rotaxane-containing nanoparticles exhibited a relatively sharp absorbance. This is attributed to the steric separation that is enforced by the surrounding rotaxane macrocycle, which prevents electronic coupling of the encapsulated croconaine. Narrow and intense NIR absorption bands are needed for eventual applications that require maximum photothermal heating or selective band irradiation.

The photothermal behaviour of the axle and rotaxane-containing nanoparticle systems were compared by irradiating separate dispersions for 20 min using either an 808 or 830 nm laser diode (250 mW) with the resulting temperature change profiles shown in Figure 12. As expected, the amount of heat generation corresponds to the relative absorbance values of the nanoparticles at the appropriate laser wavelength (Figure 11 b). Moreover, no significant changes in either the absorption spectra or DLS measurements were observed after laser irradiation (Supporting Information, Figures S53 and S54). Thus, croconaine-doped silicated micelle nanoparticles are effective water-soluble photothermal systems as they remain highly stable under laser irradiation.

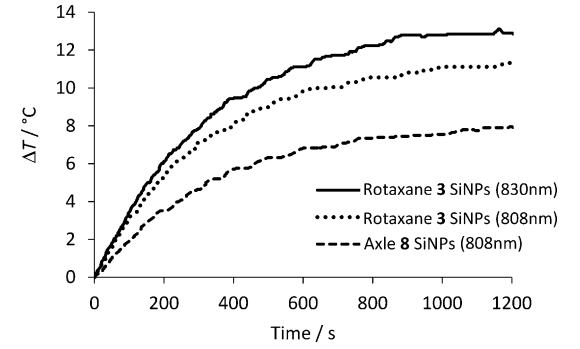


**Figure 12.** Temperature change profiles observed upon laser irradiation (250 mW, 808 or 830 nm) of solutions of silicated micelle nanoparticles (SiNPs) doped with croconaine axle **8** or rotaxane **3** ($H_2O$, 1.0 mL).

## Conclusion

The first permanently interlocked croconaine rotaxanes were successfully prepared in high yields using stoppering and clipping synthetic strategies. The stoppering approach utilised the previously reported pseudorotaxane association complex, **2**⊃**1**, while the clipping method relied on a four-component macrocyclisation around a templating croconaine axle. The use of the croconaine motif as the hydrogen bond acceptor in

a Leigh-type clipping strategy further demonstrates the synthetic versatility of this approach.[22]

At the same optical density, croconaine dye, pseudorotaxane, and rotaxane samples produce the same amount of heat under laser irradiation. Photothermal studies of organic and aqueous pseudorotaxanes found no evidence for laser-induced dethreading, and the encapsulation of a water-sensitive croconaine dye within a protective macrocycle produced a stable chromophore with a durable photothermal response. The fact that croconaine pseudorotaxanes act as robust photothermal agents that form very rapidly in water is a significant finding and supports the feasibility of future molecular designs that achieve activated photothermal heating by pseudorotaxane assembly strategies.

Along with molecular-scale systems, the hydrophobic cores of water-soluble silicated micelles were readily doped with croconaine derivatives to yield nanoparticle-scale photothermal agents with intense NIR absorptions. Axle-doped nanoparticles display band broadening owing to croconaine self-aggregation, whereas rotaxane-containing nanoparticles do not exhibit this property and thus have higher absorbance and photothermal effect. Dye encapsulation within rotaxane architectures is likely to be a general strategy for preventing any band broadening due to chromophore self-aggregation within dye-doped nanoparticles and, to the best of our knowledge, this study is the first demonstration of this approach.

## Experimental Section

### General considerations

NMR spectra were recorded on a Bruker AVANCE III HD 400, Bruker AVANCE III HD 500, and Varian DirectDrive 600 spectrometers at 295 K. High-resolution electrospray ionisation (ESI) mass spectrometry (MS) was performed using a Bruker micrOTOF II spectrometer. Commercially available solvents and chemicals were used without further purification unless otherwise stated. Water was de-ionised and microfiltered. Cu$^{I}$TBTA Br was synthesised from CuBr and TBTA,[23] and stored in a desiccator prior to use. Compounds **1**,[8a] **2**,[24] **2**⊃**1**,[8a] **7**,[18] 9,10-bis(aminomethyl)anthracene,[24] and 5-*tert*-butylisophthalic dichloride[25] were synthesised using previously reported procedures. The syntheses of compounds **4**, **6**, and **8** are given in the Supporting Information.

### Croconaine rotaxane 3

Croconaine pseudorotaxane **2**⊃**1** (17 mg, 0.012 mmol), 1-(azidomethyl)-3,5-di-*tert*-butylbenzene (**S3**;[26] 9.1 mg, 0.037 mmol), Cu$^{I}$TBTA Br (2.5 mg, 30 mol%), and DIPEA (5 μL, 0.029 mmol) were dissolved in $CHCl_3$ (3 mL) and stirred at room temperature for 24 h. The solvent was then removed in vacuo and the resulting residue purified by gradient silica gel column chromatography using 5–20% acetone/$CH_2Cl_2$ to elute the product as a black solid (20 mg, 0.010 mmol, 84%). $^1$H NMR (600 MHz, $CDCl_3$): $\delta$ = 9.23–9.59 (2H, m, $H_c$), 8.45–8.56 (4H, m, $H_b$), 7.64–8.27 (12H, m, $H_d$ and $H_f$), 7.60–7.62 (2H, m, $H_8$), 7.44–7.67 (2H, m, $H_1$), 7.40–7.41 (2H, m, $H_{11}$), 7.12–7.14 (4H, m, $H_{10}$), 6.69–7.07 (8H, m, $H_g$), 5.76–5.84 (2H, m, $H_2$), 5.51–5.54 (4H, m, $H_9$), 5.17–5.27 (8H, m, $H_e$), 4.63–4.70 (4H, m, $H_7$), 3.30–3.68 (12H, m, $H_3$ and $H_5$ and $H_6$), 1.50–1.54 (18H, m, $H_a$), 1.26–1.29 (36H, m, $H_{12}$), 1.20 ppm (6H, t, $^3J$ = 7.2 Hz, $H_4$); $^{13}$C NMR (151 MHz, $CDCl_3$): $\delta$ = 184.7, 184.3, 183.4, 182.9, 182.2, 172.3, 167.2, 166.8, 166.7, 166.5, 166.0, 152.7, 152.6, 152.5, 152.3, 151.8, 144.0, 143.9, 143.9, 139.9, 133.6, 133.6, 133.4, 133.1, 133.1, 133.0, 133.0, 132.9, 132.4, 130.5, 130.4, 130.4, 130.3, 130.3, 130.2, 129.4, 129.2, 129.2, 129.1, 129.1, 129.0, 128.9, 128.9, 128.8, 128.7, 128.4, 128.1, 126.4, 126.1, 125.9, 125.7, 125.6, 125.6, 124.6, 124.5, 124.4, 124.3, 124.2, 124.1, 123.8, 123.8, 123.5, 123.1, 122.9, 122.9, 122.9, 122.8, 122.7, 122.5, 122.5, 122.4, 113.1, 112.9, 112.7, 112.4, 67.0–67.1, 64.4, 64.4, 63.5, 54.8, 53.7, 38.1, 38.1, 37.8, 37.6, 37.3, 35.4, 35.3, 35.3, 35.3, 35.3, 34.9, 34.8, 34.8, 31.7, 31.5, 31.4, 31.4, 31.3, 31.3, 31.3, 29.7, 29.2, 15.2, 14.1, 12.1–12.3 ppm. MS-ESI *m/z* 1860.9793 ($[M+H]^+$, $C_{113}H_{127}N_{12}O_9S_2$, calcd 1860.9316), 1882.9510 ($[M+Na]^+$, $C_{113}H_{126}N_{12}NaO_9S_2$, calcd 1882.9143). $\lambda_{abs,max}$ ($CHCl_3$) 824 nm. $\varepsilon$ ($CHCl_3$) $1.8\times10^5$ L mol$^{-1}$ cm$^{-1}$. $\lambda_{em,max}$ ($CHCl_3$) 837 nm. $\Phi_f$ ($CHCl_3$) 0.02.

### Croconaine rotaxane 5

9,10-Bis(aminomethyl)anthracene[24] (71 mg, 0.30 mmol) and $Et_3N$ (0.08 mL, 0.60 mmol) were dissolved in anhydrous $CHCl_3$ (30 mL). 5-*tert*-butylisophthalic dichloride[25] (78 mg, 0.30 mmol) was dissolved in anhydrous $CHCl_3$ (30 mL). Both solutions were then added dropwise to a stirred solution of tetraalkyne croconaine dye **4** (19 mg, 0.03 mmol) in dry $CHCl_3$ (40 mL) over 8 h and the reaction mixture stirred for a further 7 h. The mixture was reduced in vacuo before filtering through celite. The solvent was removed in vacuo and the resulting residue purified by silica gel column chromatography using 2% MeOH/$CH_2Cl_2$ to yield the product as a black solid (36 mg, 0.024 mmol, 81%). $^1$H NMR (600 MHz, $CDCl_3$): $\delta$ = 9.25–9.70 (2H, m, $H_c$), 8.44–8.57 (4H, m, $H_b$), 7.38–8.32 (14H, m, $H_d$ and $H_f$ and $H_1$), 6.77–7.14 (8H, m, $H_g$), 5.55–5.67 (2H, m, $H_2$), 5.16–5.31 (8H, m, $H_e$), 4.21–4.31 (8H, m, $H_5$), 3.52–3.85 (16H, m, $H_3$ and $H_4$), 2.55–2.59 (4H, m, $H_6$), 1.51–1.57 ppm (18H, m, $H_a$); $^{13}$C NMR (151 MHz, $CDCl_3$): $\delta$ = 184.2, 167.4, 167.3, 166.8, 166.7, 166.7, 166.7, 166.6, 166.6, 165.9, 153.0, 152.6, 152.6, 152.6, 152.4, 152.3, 133.4, 133.1, 133.0, 133.0, 132.8, 130.5, 130.4, 130.3, 130.3, 130.2, 130.1, 129.2, 129.2, 129.1, 129.0, 128.8, 128.7, 128.7, 128.4, 128.0, 126.6, 126.3, 126.1, 126.1, 125.8, 125.7, 125.6, 125.6, 124.5, 124.5, 124.4, 124.4, 124.1, 124.0, 124.0, 123.9, 123.6, 123.6, 122.8, 122.8, 122.1, 78.8, 78.8, 78.8, 78.8, 75.7, 75.6, 75.6, 75.6, 58.8, 58.8, 58.8, 58.7, 58.7, 38.2, 37.9, 37.8, 37.6, 37.3, 37.2, 36.8, 35.4, 35.3, 35.3, 35.3, 31.5, 31.5, 31.4, 31.4, 31.4, 31.4, 31.1, 29.7 ppm. MS-ESI *m/z* 1477.5695 ($[M+H]^+$, $C_{89}H_{85}N_6O_{11}S_2$, calcd 1477.5712). $\lambda_{abs,max}$ ($CHCl_3$) 825 nm. $\varepsilon$ ($CHCl_3$) $1.4\times10^5$ L mol$^{-1}$ cm$^{-1}$. $\lambda_{em,max}$ ($CHCl_3$) 837 nm. $\Phi_f$ ($CHCl_3$) 0.02.

### General procedure for silicated micelle nanoparticles[21d]

Pluronic F127 (30 mg) and dye (1.91 μmol) were completely dissolved in $CH_2Cl_2$ (1 mL). The solvent was then removed in vacuo and $HCl_{(aq)}$ (0.85 M, 1 mL) was added. The mixture was vigorously stirred until all of the residue was suspended, and this was gently stirred for a further 1 h. After this time, tetraethyl orthosilicate (TEOS) (54 μL, 0.24 mmol) was added and the mixture stirred for 2 h, followed by addition of diethoxydimethylsilane (DEDMS) (4.5 μL, 26.3 μmol) and stirring for 20 h. The mixture was then transferred to dialysis tubing (Spectra/Por membrane tubing, molecular weight cut-off 12000–14000) and dialysed against water (200 mL, changed twice every 24 h) for 6 days. The resulting suspension was then filtered successively through 0.45 μm and 0.20 μm filters (Acrodisc Syringe Filters, Pall Corporation). The resulting silicated micelle nanoparticles were characterised using dynamic light scattering and absorption spectroscopy.

## Acknowledgements

This work was supported by the NSF (USA) and a Walther Cancer Foundation Advancing Basic Cancer Research Grant (2013/14) administered by the Harper Cancer Research Institute (USA). We thank the English Speaking Union (UK) for a Postdoctoral Lindemann Fellowship (G.T.S., 2012/13), Gillian Shaw for help with nanoparticle synthesis, Dr Haifeng Gao for access to DLS instrumentation, and the Royal Society (UK) for a Newton International Fellowship (C.K.).

**Keywords:** dyes · nanomaterials · rotaxanes · supramolecular chemistry · template synthesis

[1] a) A. Yuan, J. Wu, X. Tang, L. Zhao, F. Xu, Y. Hu, *J. Pharm. Sci.* **2013**, *102*, 6 – 28; b) X. Huang, M. A. El-Sayed, *Alexandria Journal of Medicine* **2011**, *47*, 1 – 9; c) W. R. Chen, R. L. Adams, S. Heaton, D. T. Dickey, K. E. Bartels, R. E. Nordquist, *Cancer Letters* **1995**, *88*, 15 – 19; d) G. Jori, J. D. Spikes, *J. Photochem. Photobiol. B Biol.* **1990**, *6*, 93 – 101.

[2] a) J. V. Jokerst, S. S. Gambhir, *Acc. Chem. Res.* **2011**, *44*, 1050 – 1060; b) S. Mallidi, G. P. Luke, S. Emelianov, *Trends Biotechnol.* **2011**, *29*, 213 – 221; c) L. V. Wang, S. Hu, *Science* **2012**, *335*, 1458 – 1462.

[3] a) A. B. S. Bakhtiari, D. Hsiao, G. X. Jin, B. D. Gates, N. R. Branda, *Angew. Chem. Int. Ed.* **2009**, *48*, 4166 – 4169; b) S. J. Leung, M. Romanowski, *Theranostics* **2012**, *2*, 1020 – 1036; c) M. Delcea, N. Sternberg, A. M. Yashchenok, R. Georgieva, H. Bäumler, H. Möhwald, A. G. Skirtach, *ACS Nano* **2012**, *6*, 4169 – 4180.

[4] H.-C. Huang, C. R. Walker, A. Nanda, K. Rege, *ACS Nano* **2013**, *7*, 2988 – 2998.

[5] C. Vázquez-Vázquez, B. Vaz, V. Giannini, M. Perez-Lorenzo, R. A. Alvarez-Puebla, M. A. Correa-Duarte, *J. Am. Chem. Soc.* **2013**, *135*, 13616 – 13619.

[6] A. Herrmann, K. Müllen, *Chem. Lett.* **2006**, *35*, 978 – 985.

[7] a) Z. Qin, J. C. Bischof, *Chem. Soc., Rev.* **2012**, *41*, 1191 – 1217; b) L. C. Kennedy, L. R. Bickford, N. A. Lewinski, A. J. Coughlin, Y. Hu, E. S. Day, J. L. West, R. A. Drezek, *Small* **2011**, *7*, 169 – 183; c) S. Lal, S. E. Clare, N. J. Halas, *Acc. Chem. Res.* **2008**, *41*, 1842 – 1851.

[8] a) G. T. Spence, G. V. Hartland, B. D. Smith, *Chem. Sci.* **2013**, *4*, 4240 – 4244; b) R. Jiang, S. Cheng, L. Shao, Q. Ruan, J. Wang, *J. Phys. Chem. C* **2013**, *117*, 8909 – 8915.

[9] a) S. Mathew, T. Murakami, H. Nakatsuji, H. Okamoto, N. Morone, J. E. Heuser, M. Hashida, H. Imahori, *ACS Nano* **2013**, *7*, 8908 – 8916; b) C. S. Jin, J. F. Lovell, J. Chen, G. Zheng, *ACS Nano* **2013**, *7*, 2541 – 2550; c) M. B. Zheng, C. X. Yue, Y. F. Ma, P. Gong, P. F. Zhao, C. F. Zheng, Z. H. Sheng, P. F. Zhang, Z. H. Wang, L. T. Cai, *ACS Nano* **2013**, *7*, 2056 – 2067; d) C. X. Yue, P. Liu, M. B. Zheng, P. F. Zhao, Y. Q. Wang, Y. F. Ma, L. T. Cai, *Biomaterials* **2013**, *34*, 6853 – 6861; e) S. Srinivasan, R. Manchanda, A. Fernandez-Fernandez, T. J. Lei, A. J. McGoron, *J Photoch Photobio B* **2013**, *119*, 52 – 59; f) L. Cheng, W. W. He, H. Gong, C. Wang, Q. Chen, Z. P. Cheng, Z. Liu, *Adv. Funct. Mater.* **2013**, *23*, 5893 – 5902; g) C. F. Zheng, M. B. Zheng, P. Gong, D. X. Jia, P. F. Zhang, B. H. Shi, Z. H. Sheng, Y. F. Ma, L. T. Cai, *Biomaterials* **2012**, *33*, 5603 – 5609; h) L. Cheng, K. Yang, Q. Chen, Z. Liu, *ACS Nano* **2012**, *6*, 5605 – 5613; i) K. Yang, H. Xu, L. Cheng, C. Y. Sun, J. Wang, Z. Liu, *Adv. Mater.* **2012**, *24*, 5586 – 5592; j) C. L. Peng, Y. H. Shih, P. C. Lee, T. M. H. Hsieh, T. Y. Luo, M. J. Shieh, *ACS Nano* **2011**, *5*, 5594 – 5607.

[10] a) S. Yasui, M. Matsuoka, T. Kitao, *Dyes Pigm.* **1989**, *10*, 13 – 22; b) X. Z. Song, J. W. Foley, *Dyes Pigm.* **2008**, *78*, 60 – 64.

[11] a) J. P. Sauvage, C. Dietrich-Buchecker, *Molecular Catenanes, Rotaxanes and Knots: a Journey Through the World of Molecular Topology*, Wiley-VCH, Weinheim, **1999**; b) X. Ma, H. Tian, *Rotaxanes-Self-Assembled Links in Supramolecular Chemistry: From Molecules to Nanomaterials*, Wiley, Hoboken, **2012**.

[12] Despite many attempts, crystals suitable for structural determination analysis have not been obtained for any thiophene–croconaine dye or rotaxane system. It is postulated that the distinct croconaine conformational isomers may be a major factor contributing to these difficulties.

[13] J. J. Gassensmith, J. M. Baumes, B. D. Smith, *Chem. Commun.* **2009**, 6329 – 6338.

[14] C. G. Collins, E. M. Peck, P. J. Kramer, B. D. Smith, *Chem. Sci.* **2013**, *4*, 2557 – 2563.

[15] K. Rurack, M. Spieles, *Anal. Chem.* **2011**, *83*, 1232 – 1242.

[16] A. M. Brouwer, *Pure Appl. Chem.* **2011**, *83*, 2213 – 2228.

[17] At 5 μM in chloroform, the pseudorotaxane partially dethreads over several days, leading to decreased absorption at 820 nm (Supporting Information, Figure S51). Thus, any laser-accelerated pseudorotaxane dissociation was expected to result in decreased absorbance and thus decreased photothermal heating. However, this was not observed.

[18] C. Ke, H. Destecroix, M. P. Crump, A. P. Davis, *Nature Chem.* **2012**, *4*, 718 – 723.

[19] An accurate association constant for this association cannot be determined owing to the instability of the bis(guanidinium) croconaine dye. However, not all water-soluble croconaine dyes are unstable, as discussed in the Supporting Information, Section S3.

[20] a) H. Zhang, L. Liu, C. Gao, R. Sun, Q. Wang, *Dyes Pigm.* **2012**, *94*, 266 – 270; b) C. M. S. Yau, S. I. Pascu, S. A. Odom, J. E. Warren, E. J. F. Klotz, M. J. Frampton, C. C. Williams, V. Coropceanu, M. K. Kuimova, D. Phillips, S. Barlow, J.-L. Bredas, S. R. Marder, V. Millar, H. L. Anderson, *Chem. Commun.* **2008**, 2897 – 2899.

[21] a) X. D. Wang, R. J. Meier, O. S. Wolfbeis, *Angew. Chem. Int. Ed.* **2013**, *52*, 406 – 409; b) D. Genovese, S. Bonacchi, R. Juris, M. Montalti, L. Prodi, E. Rampazzo, N. Zaccheroni, *Angew. Chem. Int. Ed.* **2013**, *52*, 5965 – 5968; c) X. D. Wang, J. A. Stolwijk, T. Lang, M. Sperber, R. J. Meier, J. Wegener, O. S. Wolfbeis, *J. Am. Chem. Soc.* **2012**, *134*, 17011 – 17014; d) S. Zanarini, E. Rampazzo, S. Bonacchi, R. Juris, M. Marcaccio, M. Montalti, F. Paolucci, L. Prodi, *J. Am. Chem. Soc.* **2009**, *131*, 14208 – 14209; e) Q. S. Huo, J. Liu, L. Q. Wang, Y. B. Jiang, T. N. Lambert, E. Fang, *J. Am. Chem. Soc.* **2006**, *128*, 6447 – 6453.

[22] A. S. Lane, D. A. Leigh, A. Murphy, *J. Am. Chem. Soc.* **1997**, *119*, 11092 – 11093.

[23] B.-Y. Lee, S. R. Park, H. B. Jeon, K. S. Kim, *Tetrahedron Lett.* **2006**, *47*, 5105 – 5109.

[24] J. J. Gassensmith, E. Arunkumar, L. Barr, J. M. Baumes, K. M. DiVittorio, J. R. Johnson, B. C. Noll, B. D. Smith, *J. Am. Chem. Soc.* **2007**, *129*, 15054 – 15059.

[25] A. Bugarin, B. T. Connell, *Organometallics* **2008**, *27*, 4357 – 4369.

[26] J. J. Gassensmith, L. Barr, J. M. Baumes, A. Paek, A. Nguyen, B. D. Smith, *Org. Lett.* **2008**, *10*, 3343 – 3346.

Received: April 29, 2014
Revised: June 23, 2014
Published online on August 21, 2014